

Physiological and Metabolomic Alterations in *Macrocystis pyrifera* upon Exposure to Chromium(VI)

Ying Xia Li¹, Dong Xu^{2,3}, Xiao Wen Zhang^{2,3}, Xiao Fan^{2,3}, Nai Hao Ye^{2,3,*}

¹Marine Science and Engineering College, Qingdao Agricultural University, Qingdao 266109, China. E-mail:liyxl108@163.com

²Yellow Sea Fisheries Research Institute, Chinese Academy of Fishery Sciences, Qingdao 266071, China

³Function Laboratory for Marine Fisheries Science and Food Production Processes, Qingdao National Laboratory for Marine Science and Technology, Qingdao 266071, China

*[E-mail: yenh@ysfri.ac.cn]

Received 25 April 2018; revised 06 June 2018

In order to comprehensively characterize the effects of chromium (VI) on physiological and metabolomic performance of *Macrocystis pyrifera*, the sporophytes were exposed to 2 mg L⁻¹ potassium dichromate for 3 days. *M. pyrifera* sporophytes showed decreased pigment content and Chl *a* fluorescence parameters with the accumulation of Cr(VI). The carbon content was clearly increased, while the content of nitrogen, hydrogen and sulfur were little changed. Moreover, an untargeted metabolomic analysis was carried out in order to investigate the metabolic effects and to obtain a comprehensive profiling of induced metabolites during Cr stress. Absolute quantification of 14 different metabolites was obtained through GC-MS methods. The principal component analysis showed a clear separation between control and Cr treated samples. Some pathways including carbon fixation, sulfur metabolism, taurine and hypotaurine metabolism were affected by Cr (VI) stress. These findings provided valuable information to elucidate the mechanism of *M. pyrifera* upon Cr (VI) stress.

[Keywords: Chromium; *Macrocystis pyrifera*; Metabolomic analysis; Chl *a* fluorescence parameters]

Introduction

The heavy metals are not biodegradable and possess a serious problem requiring remediation. Chromium is released in the environment through human activities and different industries like leather tanning, electroplating, wood preservation, metal plating, steel manufacturing, etc. Among different oxidation states, Cr exists in stable trivalent and hexavalent form¹. Cr (VI) presented higher mobility and caused more toxic effects at lower levels than Cr (III). The hexavalent chromium exists in aqueous solution as oxyanionic entities e.g. chromate (CrO₄²⁻), bichromate (HCrO₄⁻) and dichromate (Cr₂O₇²⁻), which depend on the pH of the solution^{2,3}. Due to higher solubility, hexavalent chromium enters into the living cells more easily and generates reactive oxygen species (ROS), causing severe oxidative injuries to cell constituents. Cr is biologically non-essential and toxic above certain threshold levels. Even with this increase in studies regarding Cr toxicity in the photosynthetic apparatus, there is still much to be done in order to fully understand the extent of effects of Cr in photosynthesis and metabolism.

Metabolomics can measure endogenous or exogenous low-molecular weight biomolecules from cells or tissues by nuclear magnetic resonance (NMR) or gas/liquid chromatography–mass spectrometry⁴. These techniques allow for a quantitative assessment of metabolic disturbances. Metabolic profiling may provide considerable insight into dysregulated metabolic pathways and physiological alterations caused by external stressors⁵. Metabolic fingerprints can be obtained using gas chromatography mass spectrometry (GC-MS), liquid chromatography- mass spectrometry (LC-MS), or nuclear magnetic resonance (NMR)⁶. Very limited studies have been performed to recognize the modulation of differential metabolomic pathway during Cr stress. In this study, the metabolomic profile variations after Cr (VI) treatment using GC-MS analysis are also investigated which provided valuable clues and insights to guide future studies on chromium stress.

Brown algae are sessile macro-organisms with great ecological relevance in coastal ecosystems. They belong to an evolutionary lineage, which have diverged from land plants and other multicellular organisms through secondary endosymbiosis more

than one billion years ago⁷. Most of these seaweeds grow in the intertidal zone where they must face marine pollutants such as heavy metals resulting from human activities. *Macrocystis pyrifera* is giant and highly productive brown seaweed of temperate coastlines in the northern and southern pacific⁸. Now, the alga is successively cultured in China. The alga can absorb the heavy metal in seawater, which resulted in series of physiological changes. The aim of the present research is to analyze the effects of Cr (VI) in several aspects of photosynthesis and metabolomics using *M. pyrifera* as model species. The following biomarkers were used to assess the Cr (VI) toxicity in photosynthesis: pigment content and Chl *a* fluorescence parameter. Until now, a comprehensive analysis of metabolites in *M. pyrifera* exposed to Cr stress has not been performed. The metabolites can be used to develop biomarkers to analyze metabolic changes and to provide ideas to relieve Cr stress in algae.

Material and Methods

Sample preparation

The sporophytes of *M. pyrifera* were initially collected in Santo tomas, Mexico (MST, 31°33' N, 116°24'W) in 1978. The male and female gametophyte clones of the lineage used were separated and kept in the Yellow Sea Fisheries Research Institute Algae Culture Center, Qingdao, China in this study. Juvenile sporophytes about 10 cm length were obtained as described in Xu *et al*⁹. using gametophyte clones and cultured in the coastline of Sungo Bay, China (SGB, 37°06' N, 122°33' E). Before the experiments, the sporophytes were collected from the coastline and washed with seawater for three times, then treated with 0 or 2 mg L⁻¹ K₂Cr₂O₇ for 72 h. After that, the alga was collected for further analysis.

Heavy metal content measurement

For determination of calcium, magnesium and chromium contents, sporophytes were washed thoroughly with distilled water for three times and dried at 60 °C for 48 h, then incinerated at 500 °C for 5 h in muffle. The obtained ash was rinsed with HNO₃ at 150 °C for 5 h. The content of Ca, Mg and Cr were analyzed using atomic absorption spectrophotometer (AAS).

Pigments content

The chlorophylla, Chlc and fucoxanthin (Fx) contents were measured using spectrophotometer.

One-tenth weight of giant kelp *M. pyrifera* was homogenized using a mortar and pestle in 2 ml of 80 % acetone at 4 °C. The resulting suspension was centrifuged at 10,000 g for 10 min. The supernatant was collected for in vivo absorption spectra measurement at room temperature.

Chlorophyll Fluorescence Measurement

Chlorophyll *a* fluorescence parameters were measured in sporophytes of *M. pyrifera* by the pulse amplitude modulated (PAM) technique and a Dual-PAM-100 instrument according the method of Xu *et al*¹⁰. The minimum (F₀) and maximum fluorescence (F_m) were measured after a dark acclimation period of 15 min. F_m yield was the real-time fluorescence yield of the sample represented as F_m' and F_t. The PSII maximum quantum yield was calculated as F_v/F_m, where F_v was the variable fluorescence emission (F_m - F₀). The relative electron transport rate (rETR) was calculated as rETR = Y(II) × PAR × 0.5, where PAR was the photosynthetic actinic radiation and 0.5 was assumed that 50 % of the absorbed light was distributed to PSII. The content of carbon, nitrogen, hydrogen and sulfur were measured with elemental analyzer (Vario MICRO cube, Elementar Company). The sporophytes of *M. pyrifera* was dried at 60 °C for 48 h, then 0.1g sample was directly placed in a 95 °C - 115 °C quartz combustion tube and burned instantaneously. After that, the content of carbon, nitrogen, hydrogen and sulphur were calculated directly by computer according to the weight of the input sample and the peak area of the signal.

GC-MS based metabonomic analysis

Fifty mg *M. pyrifera* was extracted with 0.4 mL extraction liquid (V_{methanol}: V_{H₂O} = 3: 1) and adonitol (2 mg mL⁻¹ stock in dH₂O) was added as internal standard. Then, the sample was homogenized by ultrasound for 5 min and centrifuged for 15 min at 10000 g at 4 °C. The supernatant was transferred into a fresh GC/MS glass vial and dried in a vacuum concentrator without heating. 20 µL methoxyamination hydrochloride (20 mg mL⁻¹ in pyridine) was added and incubated for 30 min at 80 °C. Thirty µL of the BSTFA reagent (1 % TMCS, v/v) was then added to the sample aliquots and incubated for 2 h at 70 °C. GC-MS analysis was performed using an Agilent 7890 gas chromatograph system coupled with a Pegasus HT time-of-flight mass spectrometer. The system utilized a DB-5MS capillary column coated with 5 % diphenyl cross-

linked with 95% dimethylpolysiloxane (30 m×250 µm inner diameter, 0.25 µm film thickness, J&W Scientific, Folsom, CA, USA). A 2 µL aliquot of the analyte was injected in splitless mode. Helium was used as the carrier gas, the front inlet purge flow was 3 mL min⁻¹, and the gas flow rate through the column was 1 mL min⁻¹. The initial temperature was kept at 50 °C for 1 min, then raised to 300 °C at a rate of 10 °C min⁻¹, then kept for 4 min at 300 °C. The injection, transfer line, and ion source temperatures were 280, 270, and 220 °C, respectively. The energy was -70 eV in electron impact mode. The mass spectrometry data were acquired in full-scan mode with the m/z range of 50-500 at a rate of 20 spectra per second after a solvent delay of 460 s.

Construction of the metabolic network map and statistical analysis

Chroma TOF4.3X software of LECO Corporation and LECO-Fiehn Rtx5 database were used for raw peaks exacting, the data baselines filtering and calibration of the baseline, peak alignment, deconvolution analysis, peak identification and integration of the peak area¹¹. The RI (retention time index) method was used in the peak identification, and the RI tolerance was 5000. The identified metabolites were mapped onto general biochemical pathways according to annotations in KEGG (<http://www.kegg.jp>) and Metaboanalyst (<http://www.ebi.ac.uk/metabolights/analysis>). Multivariate statistics was made using the Soft Independent Modeling of Class Analogy (SIMCA)-P (version 11.0, Umetrics AB, Umea, Sweden). All variables were UV (Unit Variance) scaled prior to principal component analysis (PCA) and partial least squares discriminant analysis (PLS-DA). The notable metabolite differences were screened by the loading plot in PCA and PLS-DA. Variables with VIP (Variable Importance in the Projection) >1 which played significant roles in the classification, were selected for further analysis. Subsequently, independent t-test was utilized to exclude the variables that were not significantly different ($P > 0.05$) by SPSS 16.0 software.

Results

The content of heavy metal and pigment content

Total Cr, calcium and magnesium accumulated in sporophytes of *M. pyrifera* after treated with 2 mg L⁻¹ Cr and control were shown in Table 1. The content of Cr was significantly increased after treatment with

2 mg L⁻¹ Cr in sporophytes of *M. pyrifera*, whereas, the content of Mg and Ca decreased with the increase of Cr. This result demonstrated that the accumulation of Cr affected the Ca and Mg ion uptake in sporophytes of *M. Pyrifera* indicating that Cr stress might significantly interfere with uptake, translocation, and accumulation of nutrients. The inhibition of Mg and Ca ion uptake under Cr assimilation blocked binding sites of transport proteins¹². Many studies have determined the negative effect of Cr on the uptake of nutrients, such as Zn, Fe, Ca, Mg, Mn, and Cu^{13,14,15}.

Photosynthetic pigment content was considered as a sensitive parameter under metal stress conditions as a potential biomarker for heavy metal stress¹⁶. Degradation of the photosynthetic pigments was routinely observed in response to exposure of plants to various heavy metals. Cr could degrade δ-aminolevulinic acid dehydratase, an important enzyme involved in chlorophyll biosynthesis, thereby affecting pigment content¹⁷. The content of Chla, *chl c* and Fx in *M. pyrifera* were illustrated in Fig 1. The content of *chl a* and fucoxanthin were clearly decreased in *M. pyrifera* under Cr stress. This loss of pigments causes deficiency in light-harvesting

Table 1 — Total Cr, Ca and Mg accumulated in sporophytes in *M. pyrifera* exposed to 0 or 2 mg L⁻¹ Cr for 72 h. Three replicates were performed, and values given as the mean± SD.

	Cr (µg L ⁻¹)	Ca (mg L ⁻¹)	Mg (mg L ⁻¹)
Ck	3.21±0.68	7.24±0.86	4.50±0.12
2 mg L ⁻¹ Cr	23.87±2.18*	6.05±0.09*	4.01±0.34*

*Different letters in the same column represent a significant difference at 95% probability in *M. pyrifera* exposed 2 mg L⁻¹ Cr for 72h with comparison with the control.

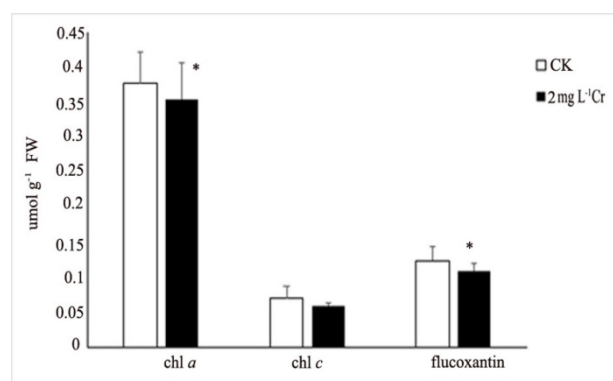


Fig. 1 — Chl a, *chl c* and fucoxanthin levels for *M. pyrifera* exposed to 0 or 2 mg L⁻¹ Cr for 72 h. *Different letters in the same column represent a significant difference at 95% probability in *M. pyrifera* exposed 2 mg L⁻¹ Cr for 72 h with comparison with the control.

capacity¹⁸ and consequently a decrease in photosynthetic capacity of the plant.

Chlorophyll fluorescence measurement

The pulse amplitude modulation (PAM) fluorescence was a rapid and non-intrusive technique to monitor photosynthetic performance of algae much earlier than the appearance of visible injury¹⁹. It was also applied in ecophysiological and toxicological studies to examine the effect of pollutants on algae²⁰. Fv/Fm parameter was a standard chlorophyll fluorescence parameter representing the maximum quantum efficiency of photosystem II. In the average Fv/Fm, the relative electron transport rate (rETR) and light utilization efficiency (α) in *M. Pyrifera* were significantly decreased under Cr stress (Table.2). Cr (VI) also proved to have deleterious effects of *M. pyrifera* in the levels of fluorescence emitted, as indicated by the rETR, Fv/Fm and α (light utilization efficiency).

The content of C, N, H and S were shown in Figure 2. The content of carbon was clearly increased, and the content of nitrogen, hydrogen and sulfur were little changed on *M. pyrifera* under Cr (VI) stress.

Table 2 — PSII photophysiological responses in *M. pyrifera* exposed to 0 or 2 mg L⁻¹ Cr for 72h. Fv/Fm: Maximum quantum yield, relative electron transport rate (rETR), light utilization efficiency (α). Three replicates were performed, and values given as the mean \pm SD.

	Fv/Fm	rETR	α
Ck	0.243 \pm 0.031	132.11 \pm 11.82	0.232 \pm 0.02
2 mg L ⁻¹ Cr	0.232 \pm 0.038*	125.72 \pm 12.11*	0.215 \pm 0.02*

*Different letters in the same column represent a significant difference at 95% probability exposed 2 mg L⁻¹ Cr for 72h with comparison with the control.

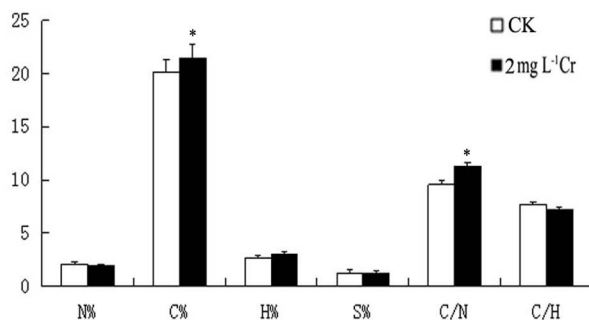


Fig. 2 — The content of carbon, nitrogen, hydrogen and sulfur in *M. pyrifera* exposed to 0 or 2 mg L⁻¹ Cr for 72h. *Different letters in the same column represent a significant difference at 95% probability in *M. pyrifera* exposed 2 mg L⁻¹ Cr for 72h with comparison with the control.

Metabolites in *M. pyrifera* determined by GC-MS

The primary metabolites were characterized using the GC-MS data in this study, which can provide a fundamental view of the changes due to *M. pyrifera* exposure to Cr. A total of 341 metabolites were detected by GC-MS and 14 different metabolites including 1,3-diaminopropane, 2-monopalmitin and tyrosine, 1-monopalmitin, 2-hydroxy-3-isopropylbutanedioic acid, aminomalonic acid, beta-glutamic acid, cumic acid, glucoheptonic acid, ornithine, serine, sorbitol, sulfuric acid were identified in *M. pyrifera* after Cr treatment. Among these, 1,3-diaminopropane, 2-monopalmitin and tyrosine were clearly increased, while 1-monopalmitin, 2-hydroxy-3-isopropylbutanedioic acid, aminomalonic acid, beta-glutamic acid, cumic acid, glucoheptonic acid, ornithine, serine, sorbitol and sulfuric acid were significantly decreased (Table 3).

The resulted three-dimensional dates including the peak number, sample name, and normalized peak area were fitted to SIMCA14.1 software package (Umetrics, Umea, Sweden) for principal component analysis (PCA) and orthogonal projections to latent structures-discriminate analysis (OPLS-DA). As shown in Fig. 3, the principal component analysis (PCA) showed the distribution of origin data. In PCA score plot, the Cr treatment groups were separated from control group, while no discernible clustering was observed between Cr treatment group and control group (Fig. 3A). The PLS-DA was applied to better understand the different metabolic patterns. The OPLS-DA model was established using two components and had R² and Q² values of 0.918 and 0.013, respectively. The principal component analysis (PCA) showed a separation among samples within the control and Cr treatment samples (B).

In order to analyze the potential pathways of *M. pyrifera* to Cr stress, a free and web-based tool (MetaboAnalys) was utilized for pathway analysis (<http://www.metaboanalyst.ca>), which used the high-quality KEGG metabolic pathway as the backend knowledge base. The pathway impact value calculated from pathway topology analysis. The pathway analysis graph contained all matched metabolic pathway using the Japanese rice as the model organisms. The X axis was the metabolic pathway which impact factor pathway topology analysis. While the Y axis was obtained by the pathway enrichment analysis according to the p value of $-\log$. The color of each circle from yellow to red was

Table 3 — List of different metabolites in *M. pyrifera* exposed to 0 or 2 mg L⁻¹ Cr for 72 h.

Varid (primary)	Peak	RT	Mass	Relative peak areas (CK)	Relative peak areas (treatment)	p-value	Fold change
307	1,3-diaminopropane	17.20	174	0.001442	0.001987	0.0149	1.3779
511	1-monopalmitin	25.86	371	0.000327	0.000219	0.07908	0.6697
286	2-hydroxy-3-isopropylbutanedioic acid	16.30	275	0.000419	0.000175	0.09194	0.4176
507	2-monopalmitin	25.56	387	0.000758	0.002141	0.09997	2.8245
252	Aminomalonic acid	14.98	218	0.000430	0.000063	0.04857	0.1465
297	beta-Glutamic acid	16.71	73	0.003476	0.001880	0.02575	0.5409
272	Cumic Acid	15.84	292	0.000155	0.000086	0.00445	0.5548
435	Glucoheptonic acid	22.15	292	0.000364	0.000055	0.00012	0.1511
352	Ornithine	19.03	142	0.002693	0.000674	0.0888	0.2503
211	Serine	13.59	171	0.000210	0.000076	0.07024	0.3619
387	Sorbitol	20.31	410	0.011578	0.006892	0.06104	0.5953
113	Sulfuric acid	10.73	147	0.001206	0.000199	0.00361	0.1650
391	Tyrosine	20.36	100	0.019401	0.049823	0.03425	2.5681

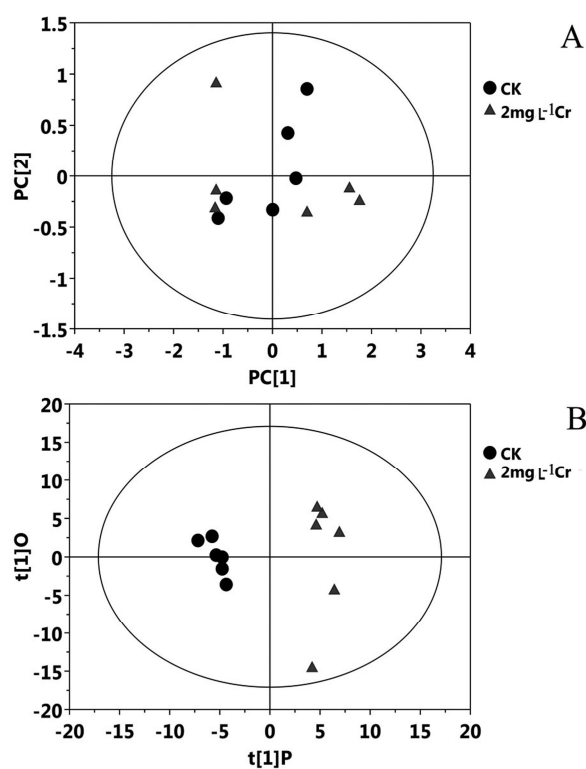


Fig. 3 — Principal component analysis (PCA) of metabolite profiles in *M. pyrifera* under control and Cr stress. The analysis was performed on all metabolites detected in *M. pyrifera* exposed to 0 or 2 mg L⁻¹ Cr for 72 h.

determined by the enrichment analysis of *P* value. The red color represented larger $-\log P$ value. The radius of each circle was laid on the topological analysis of the value, namely, larger circle showed the greater the value of impact factor. As shown in Figure 4, some pathways including carbon fixation, sulfur

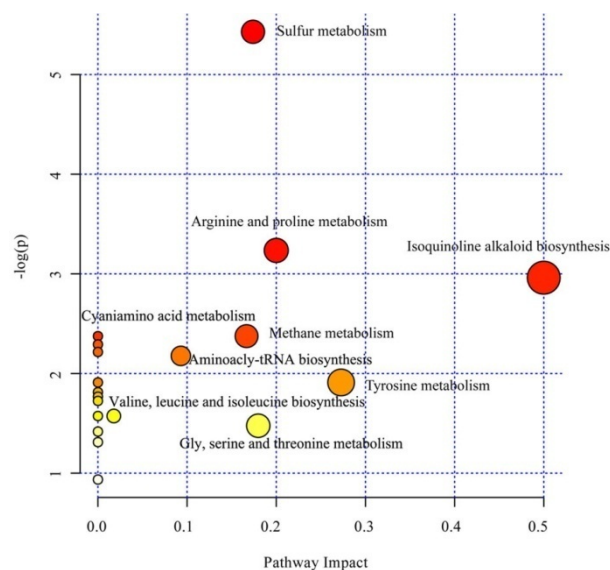


Fig. 4 — Summary of pathway analysis in *M. pyrifera* under control and Cr stress. The X axis was the metabolic pathway, while the Y axis was got by the pathway enrichment analysis according to the *p* value of $-\log$.

metabolism, taurine and hypotaurine metabolism were significantly affected by Cr stress.

Discussion

The decreased Fv/Fm might be a result of photo-inhibition or other injury to PSII components in rice seedlings under Cr (VI) stress^{21,22}. Higher Cr might decrease Fv/Fm and degrade the electron transfer system of *Euglena gracilis*, *Scenedesmus obliquus* and *Chlorella pyrenoidosa*, thereby impairing electron transfer between PSII and PSI^{23,24}. While Takami *et al.*²⁵ also reported that concentrations

higher than 1 mg L^{-1} caused a significant increase in the electron transfer rates (ETR) and photosystem II quantum yields in *Monoraphidium convolutum* after a short-term (2 h) of exposure, and there was a subsequent decline in both parameters after 48 and 72 h. Above results showed that the effects of Cr on chlorophyll fluorescence parameters depend on the concentration and time of treatment. This together with the data for pigment content suggested that at this concentration the photochemical apparatus might have been compromised with the lower amount of pigments than that of control.

The increase in carbon content under Cr(VI) stress on *M. pyrifer* suggested that carbon fixation was significantly changed with the accumulation of Cr(VI). Amino acids (AAs) might play an important role in plant stress resistance through osmotic adjustment and the accumulation of compatible osmolytes, detoxification of ROS and pH regulation²⁶. The interruption in nutrient metabolism consequently lead to AAs loss, while some stress responsive AAs viz., proline, cysteine and glycine were known to be induced significantly during As exposure^{27,28}. Serine and glutamic acid were clearly decreased, whereas tyrosine and ornithine were significantly increased in *M. pyrifer* under Cr(VI) stress in the present study. Other metabolites such as 1, 3-diaminopropane, 2-monopalmitin et al. were changed under Cr(VI) stress suggesting that metabolic changes were induced by Cr(VI) in *M. pyrifer*.

Conclusion

The pigment content and Chl *a* fluorescence parameters were decreased on *M. pyrifer* sporophytes after being treated with 2 mg.L^{-1} Cr(VI) for 3 days. The carbon content was clearly increased, while the content of nitrogen, hydrogen and sulfur were little changed. Fourteen different metabolites were analyzed using an untargeted metabolomic analysis. The principal component analysis showed a clear separation between control and Cr(VI) treated *M. pyrifer*. Some pathways such as carbon fixation, sulfur metabolism, taurine and hypotaurine metabolism were changed under exposure to Cr(VI). Above results suggested that physiological and metabolic changes was induced by Cr(VI) on *M. pyrifer*.

Acknowledgement

The work is supported by National Natural Science Foundation of China (41501533, 41676145) and

"First class fishery discipline" programme in Shandong Province, China.

References

- James, B. R., & Bartlett, R. J., Behavior of chromium in soils. VI. Interactions between oxidation-reduction and organic complexation, *J. Environ. Qual.*, 12: (1983), 173-176.
- Das, S. K., Das, A. R., & Guha, A. K., Structural and nanomechanical properties of *Termitomyces clypeatus* cell wall and its interaction with chromium (VI), *J. Phys. Chem. B.*, 113: (2009), 1485-1492.
- Das, S. K. & Guha, A. K., Biosorption of chromium by *Termitomyces clypeatus*, *Colloid. Surface. B: Biointerfaces*, 60: (2007), 46-54.
- Theodoridis, G., Gika, H. G., & Wilson, I. D., Mass spectrometry-based holistic analytical approaches for metabolite profiling in systems biology studies, *Mass. Spectrom. Rev.*, 30: (2011), 884-904.
- Kuo, C. H., Wang, K. C, Tian, T. F., Tsai, M. H., Chiung, Y. M., Hsieh, C. M., Tsai, S. J., Wang, S. Y., Tsai, D. M., Huang, C. C., & Tseng, Y. J, Metabolomic characterization of laborers exposed to welding fumes, *Chem. Res. Toxicol.*, 25: (2012), 676-686.
- Nicholson, J. K., Holmes, E., Lindon, J. C., & Wilson, I. D., The challenges of modeling mammalian biocomplexity, *Nat. Biotechnol.*, 22 (10): (2004), 1268-1274.
- Cock, J. M., Peters, A. F., & Coelho, S. M., Brown algae, *Curr. Biol.*, 21: (2011), 573-575.
- Graham, M., Va'squez, J., & Buschmann, A., Global ecology of the giant kelp *Macrocystis*: from ecotypes to ecosystems, *Oceanogr. Mar. Biol.*, 45: (2007), 39-88.
- Xu, D., Ye, N. H., Cao, S. N., Wang, Y. T., Wang, D. S., Fan, X., Zhang, X. W., An, M. L., Mou, S. L., & Mao, Y. Z., Variation in morphology and PSII photosynthetic characteristics of *Macrocystis pyrifer* during development from gametophyte to juvenile sporophyte, *Aquaculture research*, 46: (2015), 1699-1706.
- Xu, D., Wang, Y. T., Fan, X., Wang, D. S., Ye, N. H., Zhang, X. W., Mou, S. L., Guan, Z., & Zhuang, Z. M., Long-Term Experiment on Physiological responses to synergetic effects of ocean acidification and photoperiod in the antarctic sea ice algae *Chlamydomonas sp.* ICE□L, *Environ. Sci. Technol.*, 48: (2014), 7738-7746.
- Tobias, K., Gert, W., Yup, L. D., Yun, L., Mine, P., Sevini, S., & Oliver, F., FiehnLib- mass spectral and retention index libraries for metabolomics based on quadrupole and time-of-flight gas chromatography/mass spectrometry, *Anal. Chem.*, 81(24): (2009), 10038-10048.
- Oh, M. W., Roy, S. K., Kamal, A. H. M., Cho, K., Cho, S. W., Park, C. S., Choi, J. S., Komatsu, S., & Woo, S. H., Proteome analysis of roots of wheat seedlings under aluminum stress, *Mol. Biol. Rep.*, 41: (2014), 671-681.
- Gardea-Torresdey, J. L., Peralta-Videa, J. R., Montes, M., de la Rosa, G., & Corral-Diaz, B., Bioaccumulation of cadmium, chromium and copper by *Convolvulus arvensis* L.: impact on plant growth and uptake of nutritional elements, *Bioresour. Technol.*, 92: (2004), 229-235.
- Zeng, F., Ali, S., Qiu, B., Wu, F., & Zhang, G., Effects of chromium stress on the subcellular distribution and chemical form of Ca, Mg, Fe, and Zn in two rice genotypes, *J. Plant. Nutr. Soil. Sci.*, 173: (2010), 135-148.

- 15 Zhang, Y. F., Wang, Y., Ding, Z. T., Wang, H., Song, L. B., Jia, S. S., & Ma, D. X., Zinc stress affects ionome and metabolome in tea plants, *Plant Physiology and Biochemistry*, 111: (2017), 18-328.
- 16 Qiao, X. Q., Shi, G. X., Chen, L., Tian, X. L., & Xu, X. Y., Lead-induced oxidative damage in steriled seedlings of *Nymphoides peltatum*. *Environ. Sci. Pollut. R.*, 20: (2013), 5047-5055.
- 17 Hayat, S., Khalique, G., Irfan, M., Wani, A. S., Tripathi, B. N., & Ahmad, A., Physiological changes induced by chromium stress in plants: an overview, *Protoplasma*, 249: (2012), 599-611.
- 18 Mazhoudi, S., Chaoui, A., Ghorbal, M. H., Ferjani, E. E., Response of antioxidant enzymes to excess copper in tomato (*Lycopersicon esculentum* Mill.), *Plant. Sci.*, 127: (1997), 129-137.
- 19 Kumar, K. S., & Han, T., Toxicity of single and combined herbicides on psii maximum efficiency of an aquatic higher plant, *Lemna sp*, *Toxicol. Environ. Health. Sci.*, 3(2): (2011), 97-105.
- 20 Kumar, K. S, Dahms, H. U., Lee, J. S, Kim, H. C, Lee, W. C & Shin, K. H, Algal photosynthetic responses to toxic metals and herbicides assessed by chlorophyll a fluorescence, *Ecotox. Environ. Safe.*, 104: (2014), 51-71.
- 21 Rodriguez, E., Santos, C., Azevedo, R., Moutinho-Pereira, J., Correia, C., & Dias, M. C., Chromium (VI) induces toxicity at different photosynthetic levels in pea, *Plant. Physiol. Biochem.*, 53: (2012), 94-100
- 22 Roháček, K., Chlorophyll fluorescence parameters: the definitions, photosynthetic meaning, and mutual relationships, *Photosynthetica* 40: (2002), 13-29.
- 23 Hörcsik, Z. T., Kovács, L., Láposi, R., Mészáros, I., Lakatos, G., & Garab, G., Effect of chromium on photosystem 2 in the unicellular green alga, *Chlorella pyrenoidosa*, *Photosynthetica*, 45(1): (2007), 65-69.
- 24 Khalida, Z., Youcef , A., Zitouni, B., Mohammed, Z., & Radovan, P., Use of chlorophyll fluorescence to evaluate the effect of chromium on activity photosystemIII at the alga *Scenedesmus obliquus*, *Int. J. Res. Rev. Appl. Sci.*, 12 (2): (2012), 304-314.
- 25 Takami, R., Almeida, J. V., Vardaris, C. V, Colepicolo, P., & Barrosa, M. P., The interplay between thiol-compounds against chromium(VI) in the freshwater green alga *Monoraphidium convolutum*: toxicology, photosynthesis, and oxidative stress at a glance, *Aquat. Toxicol.*, 118-119 (1): (2012), 80-87.
- 26 Tripathi, S. D., Singha, R., Tripathia, P., Dwivedia, S., Chauhana, R., Adhikarib, B., & Trivedia, P. K., Arsenic accumulation and tolerance in rootless macrophyte *Najas indica* are mediated through antioxidants, amino acids and phytochelatin, *Aquat. Toxicol.*, 157: (2014), 70-80.
- 27 Dwivedi, S., Tripathi, R. D., Srivastava, S., Singh, R., Kumar, A., Tripathi, P., Dave, R., Rai, U, N., Chakrabarty D, Trivedi P K, Tuli R, Adhikari B & Bag M K, Effect of arsenate exposure on amino acids, mineral nutrient status and antioxidant in rice (*Oryza sativa* L.) genotypes, *Environ. Sci. Technol.*, 44: (2010), 9542-9549.
- 28 Tripathi, P., Mishra, A., Dwivedi, S., Chakrabarty, D., Trivedi, P, K., Singh, R. P., & Tripathi, R. D., Differential response of oxidative stress and thiol metabolism in contrasting rice genotypes for arsenic tolerance, *Ecotoxicol. Environ. Saf.* 79: (2012), 189-198.